Supporting Information

In vitro and *in vivo* osteogenesis up-regulated by two-dimensional nanosheets through a macrophage-mediated pathway

Haoming Liu[1,2,#], Gaojie Yang[7,#], Hao Yin[1,2], Zhenxing Wang[1,2], Chunyuan Chen[1,2], Zhengzhao Liu[2,3], Hui Xie[1-6,]*

[1]Department of Orthopedics, Xiangya Hospital, Central South University, Changsha 410008, China

[2]Movement System Injury and Repair Research Center, Xiangya Hospital, Central South University, Changsha 410008, China

[3]Department of Sports Medicine, Xiangya Hospital, Central South University, Changsha 410008, China

[4]National Clinical Research Center for Geriatric Disorders, Xiangya Hospital, Central South University, Changsha 410008, China

[5]Hunan Key Laboratory of Organ Injury, Aging and Regenerative Medicine, Changsha 410008 China.

[6]Hunan Key Laboratory of Bone Joint Degeneration and Injury, Changsha 410008 China.

[7]Department of Materials, Huazhong University of Science and Technology, Wuhan 430074, China,

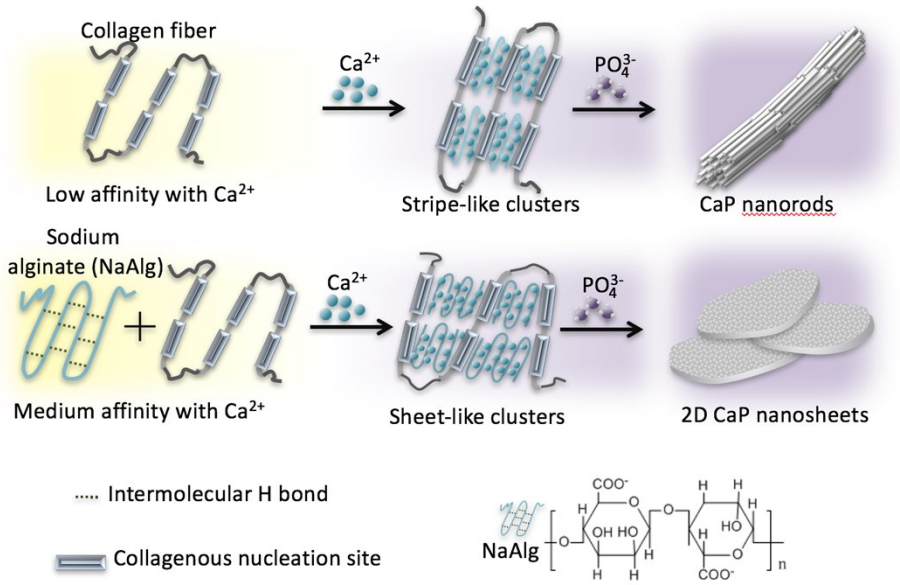

Figure S1 Template-directed biomimetic synthesis of Ca/P nanoparticles using a modified LSS method. Super-molecule structures were formed due to the interaction between carboxyl group on the molecular backbone of templates and Ca^{2+} ions, which subsequently regulate the morphology of mineralized nanoparticle during the LSS reaction.

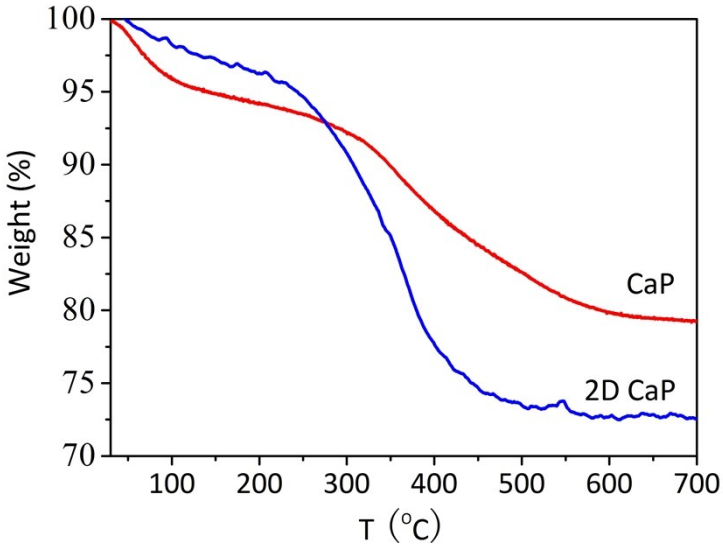

Figure S2 thermogravimetry (TG) for thermal stability and component analysis of CaP and 2D CaP nanoparticles. The data showed that both CaP and 2D CaP nanoparticles had an organic content of 75%-80%.

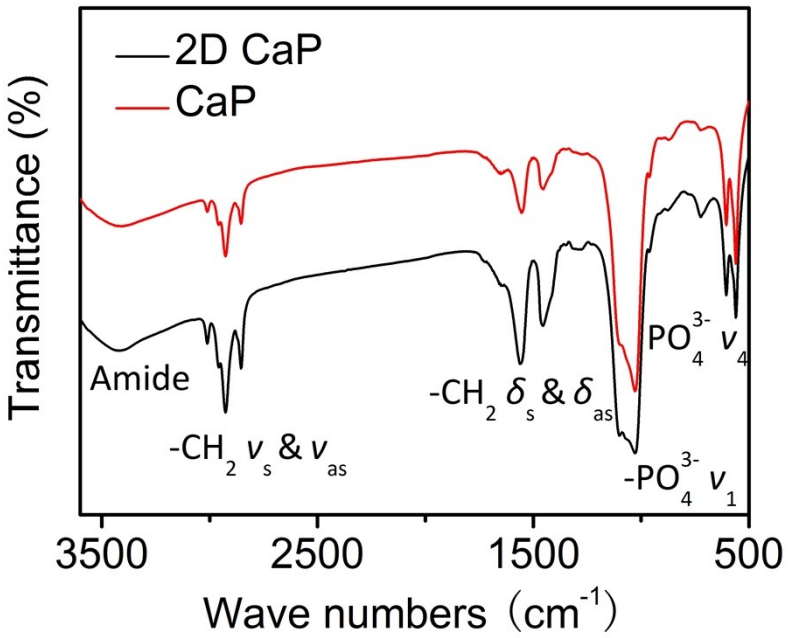

Figure S3 FT-IR spectra analysis for the CaP and 2D CaP nanoparticles, which confirmed the inorganic component in the NPs. Both NPs exhibited a similar FT-IR absorption at approximately 1027 cm^{-1}, which could be assigned to the characteristic stretching vibration for phosphate group. Besides, both of the FT-IR spectra revealed similar peaks at around 1561 cm^{-1} and 1455 cm^{-1}, which is attributed to amide group of Col and methylene on backbone of NaAlg and Col molecules.

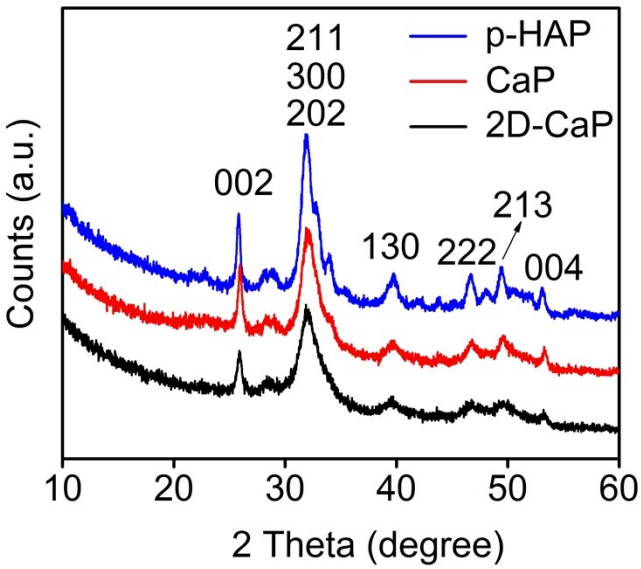

Figure S4 X-ray diffraction (XRD) analysis for the CaP, 2D CaP and pure hydroxyapatite (p-HAp) nanoparticles, which identified the crystalline component in the NPs. The diffraction patterns showed three characteristic peaks of hydroxyapatite at $2\theta = 25.9°$ (002), $2\theta = 39.5°$ (310) in all NP groups, and a overlapped peak at $2\theta = 32.8°$ for (211), (300) and (202) planes.

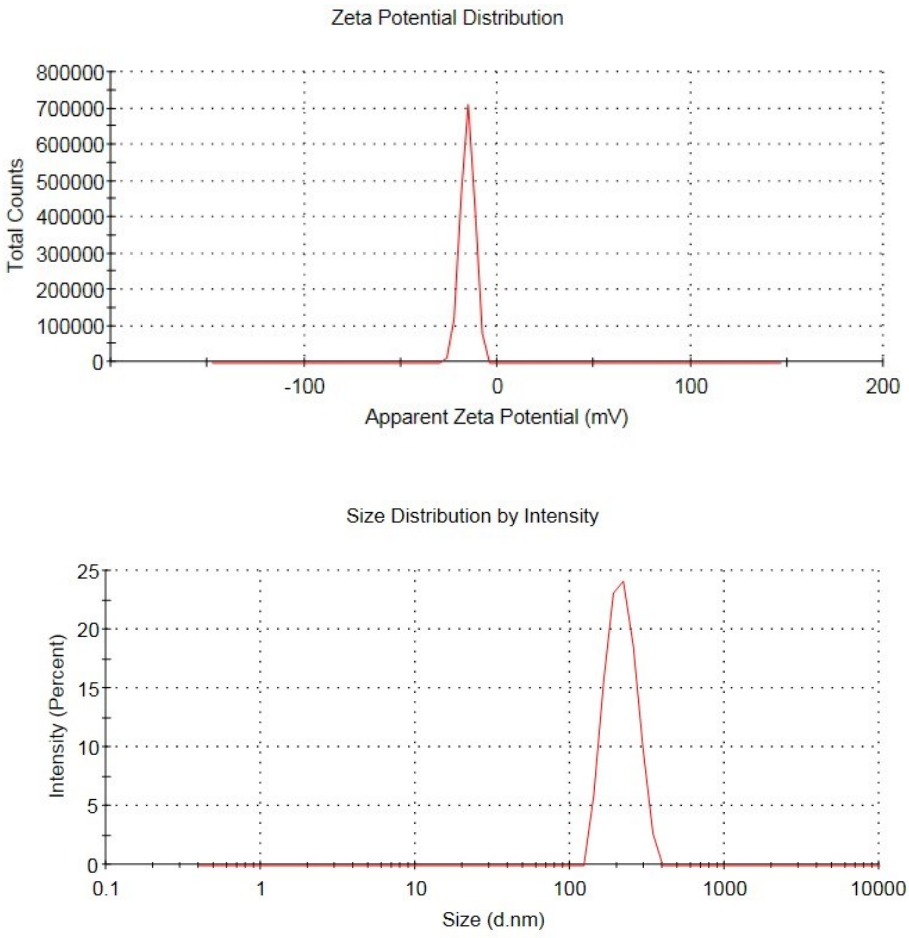

Figure S5 Zeta potential (upper) and dynamic light scattering (DLS, bottom) analysis for the as-prepared CaP nanoparticles. The CaP nanoparticles were negative charged with a zeta potential of -15.4 mV. DLS result showed that the nanoparticles were well distributed in water with an average size of 217 nm.

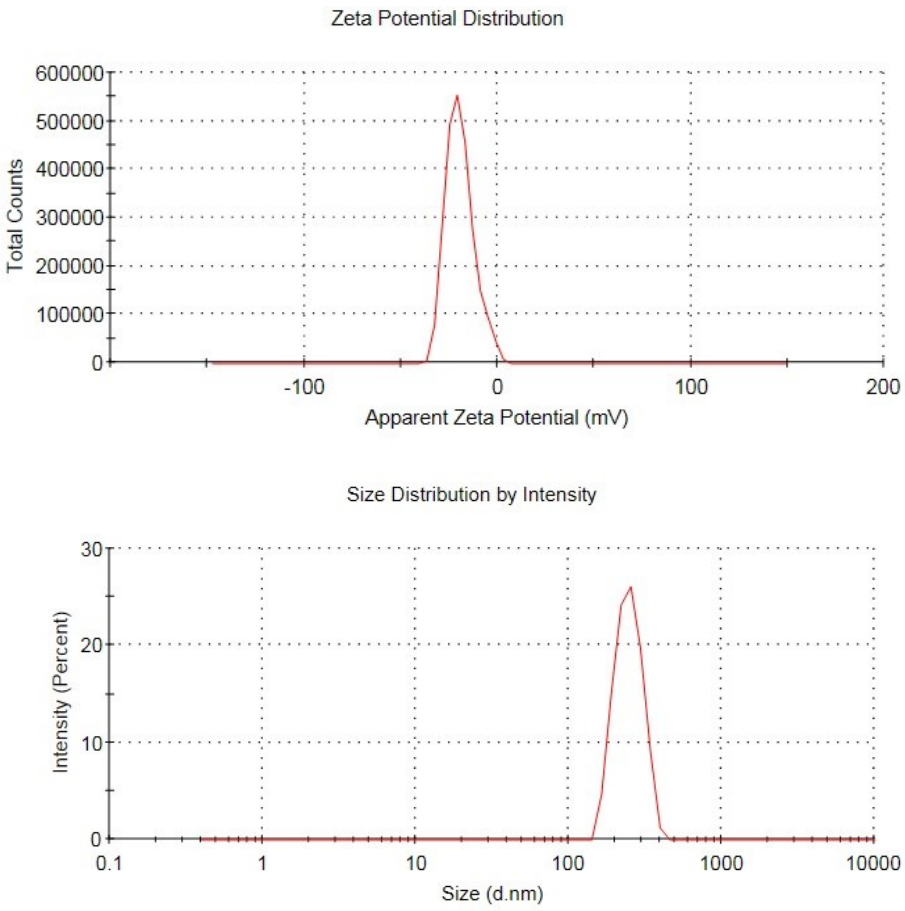

Figure S6 Zeta potential (upper) and dynamic light scattering (DLS, bottom) analysis for the as-prepared 2D CaP nanoparticles. The 2D nanoparticles were negative charged with a zeta potential of -19.4 mV. DLS result showed that the nanoparticles were well distributed in water with an average size of 250 nm.

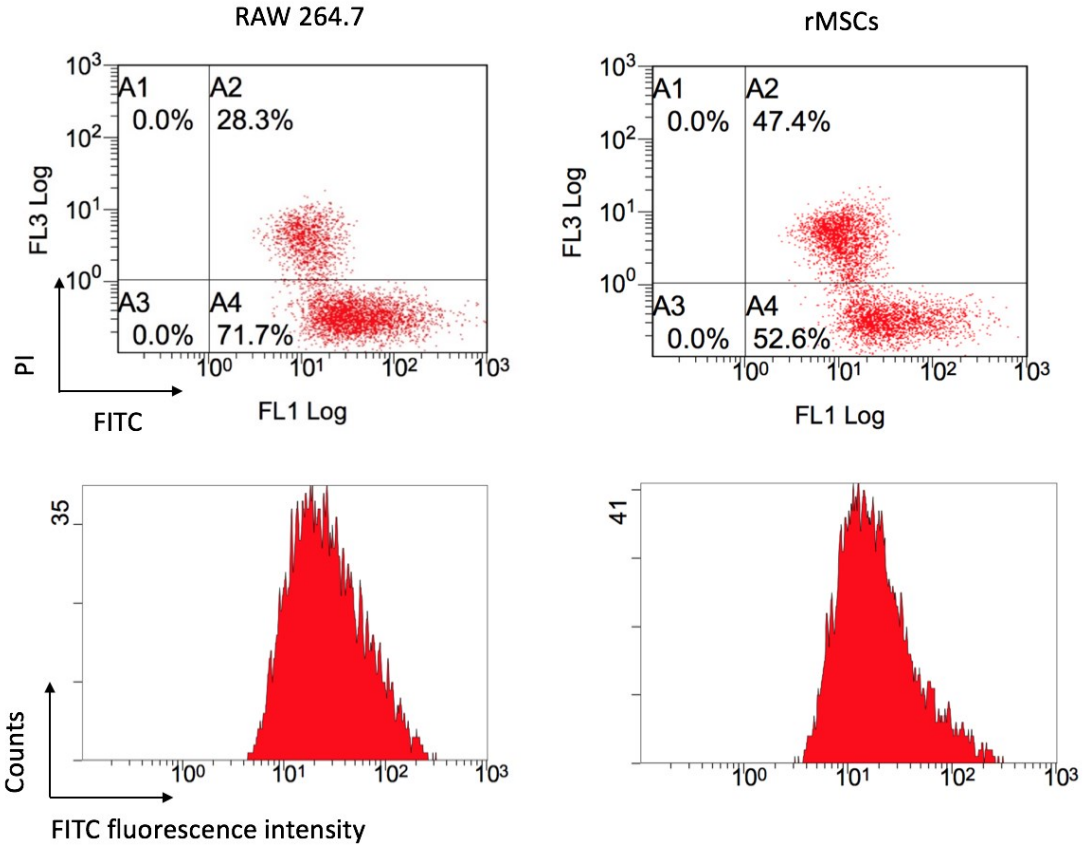

Figure S7 Fluorescence activated cell sorter (FACS) for the uptake ability of RAW 264.7 cells and rMSCs upon 2D CaP nanoparticles. The cells were treated with FITC labelled nanoparticles for overnight and cell nuclei were counter-stained red with propidium iodide (PI), before subjected to flow cytometer analysis. The result showed that almost all the cells internalized the NPs. However, much more NPs were internalized by macrophages, as suggested by higher mean fluorescence intensity (MFI) in RAW 264.7 group (45.4) than that in rMSCs group (MFI: 33.3).

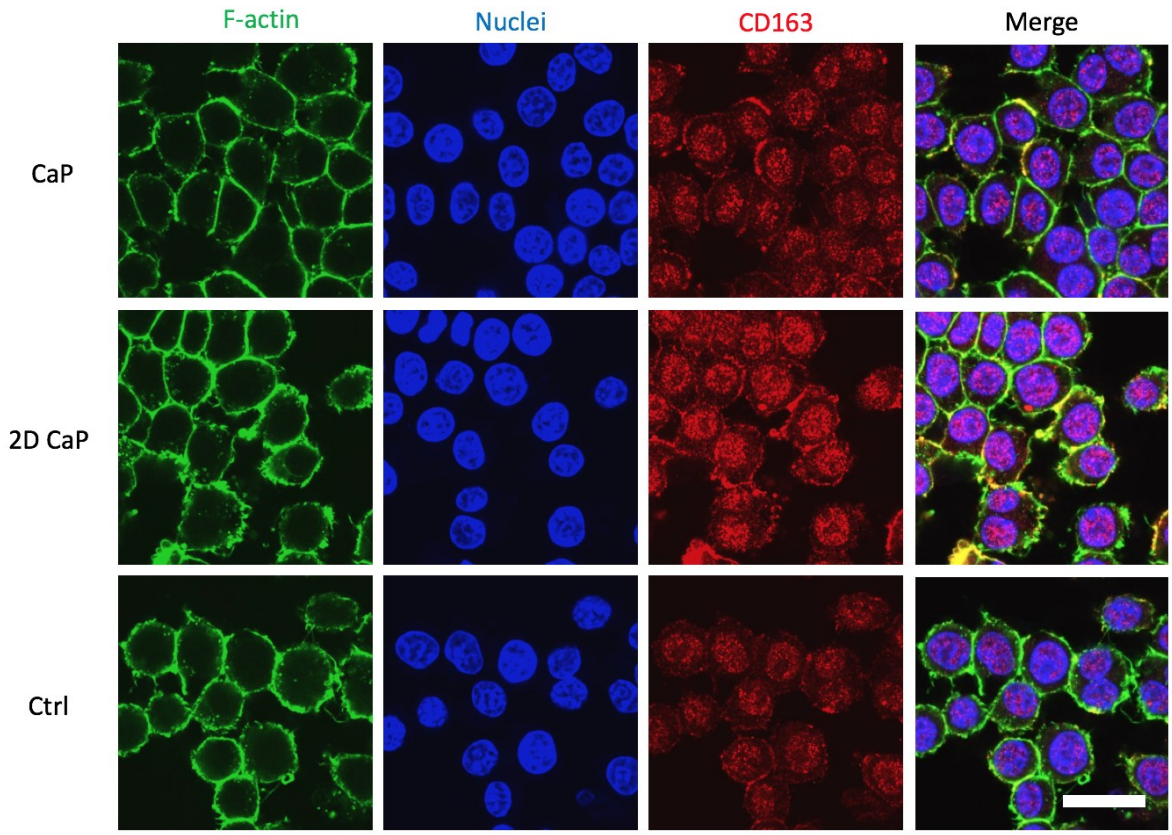

Figure S8 IF staining for the expression of polarization specific surface marker CD163 after the RAW 264.7 cells were incubated with indicated nanoparticles for 3 days. The proteins were stained with Cy3-labeled primary antibody against CD163 (red), nuclei were stained by DAPI (blue), and F-actin was stained with FITC labeled phalloidin (green). Scale bar = 50 μm.

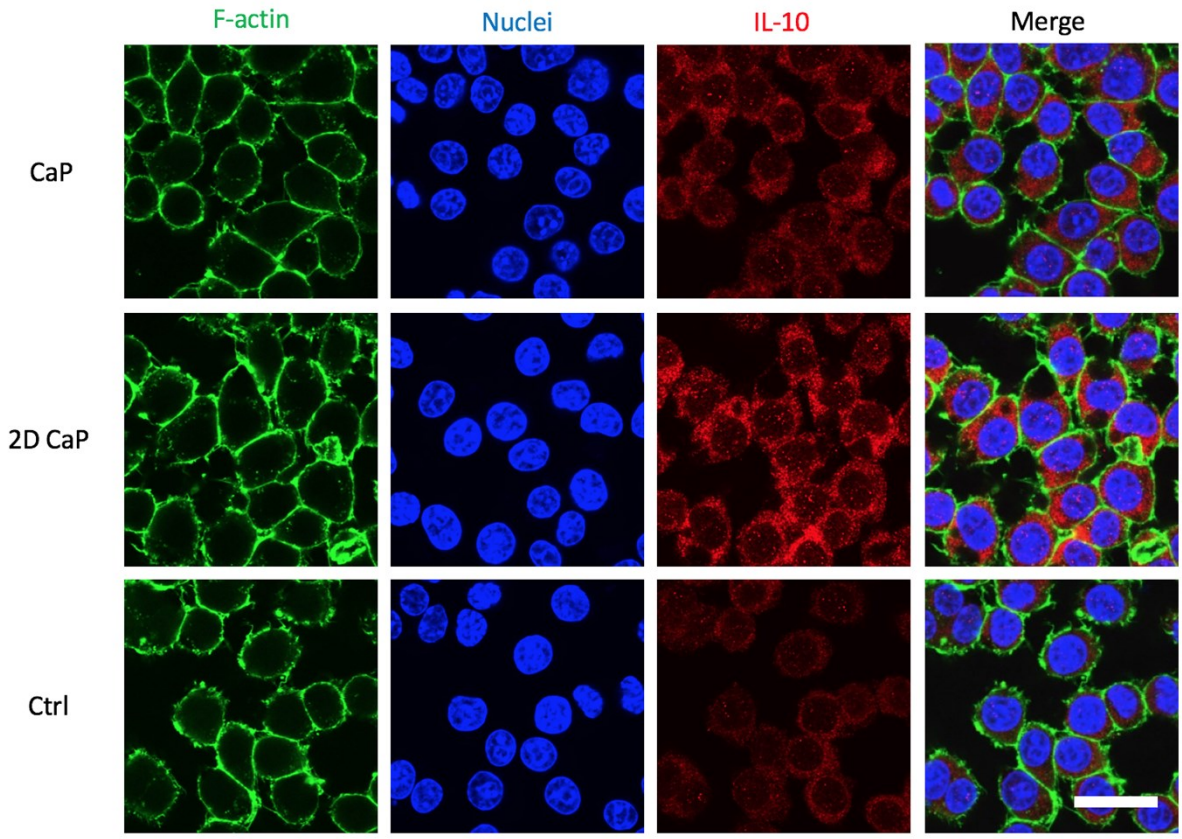

Figure S9 IF staining for the expression of polarization specific surface marker IL-10 after the RAW 264.7 cells were incubated with indicated nanoparticles for 3 days. The proteins were stained with Cy3-labeled primary antibody against IL-10 (red), nuclei were stained by DAPI (blue), and F-actin was stained with FITC labeled phalloidin (green). Scale bar = 50 μm.

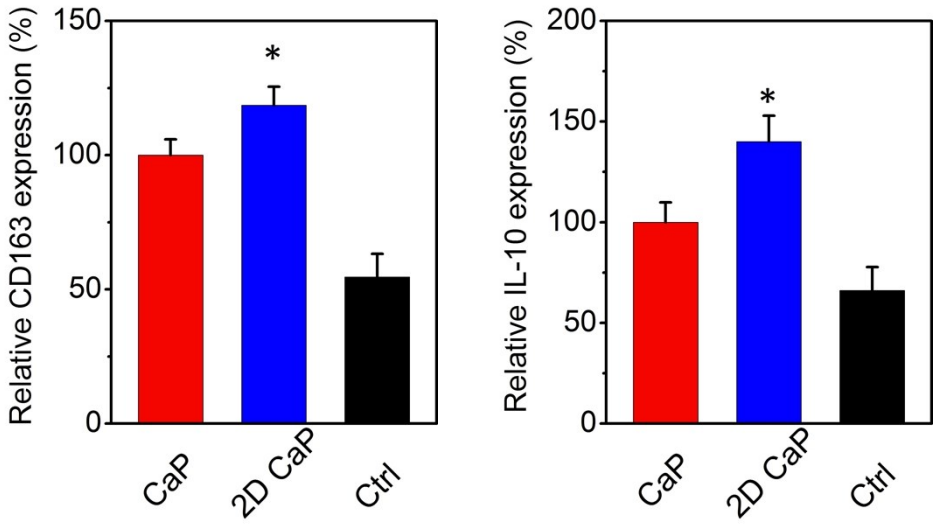

Figure S10 Relative protein contents as represented by quantifying the fluorescent intensity in corresponding IF images.

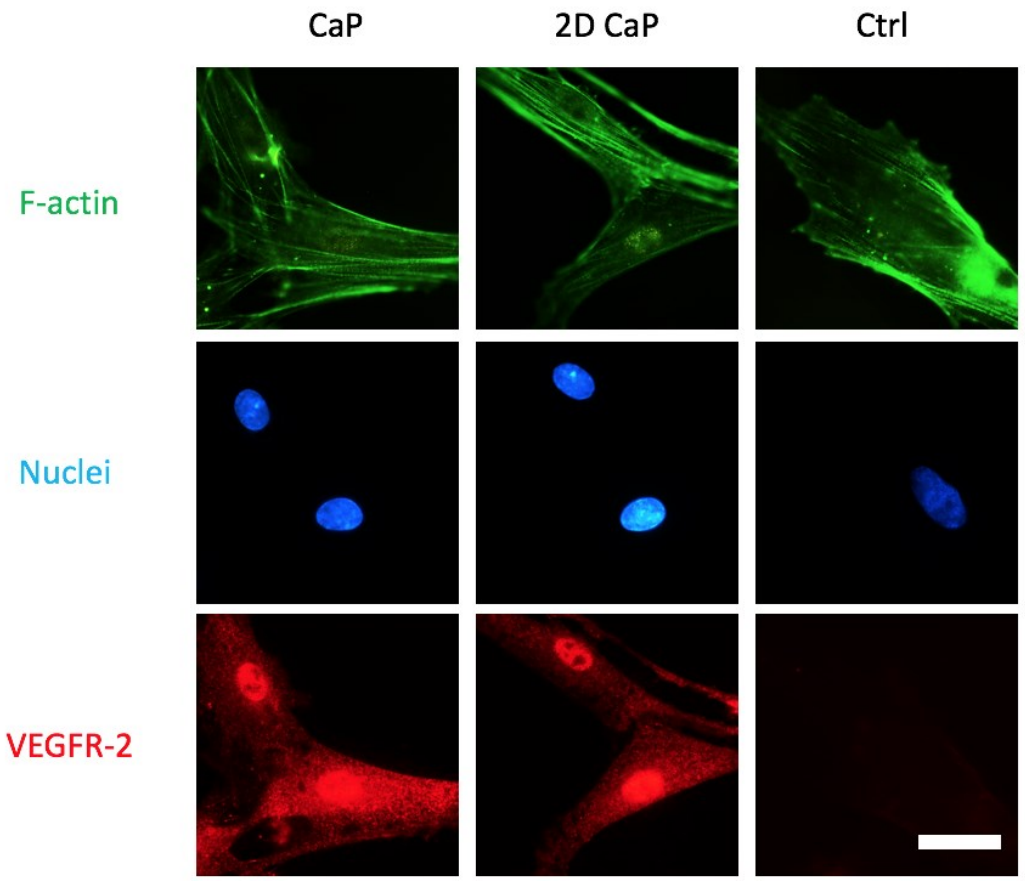

Figure S11 IF staining for the expression of angiogenic markers VEGFR-2 in rMSCs after co-cultured with polarized RAW 264.7 cells for 3 days. The proteins were stained with Cy3-labeled primary antibody (red), nuclei were stained by DAPI (blue), and F-actin was stained with FITC labeled phalloidin (green). Scale bar = 50 μm.

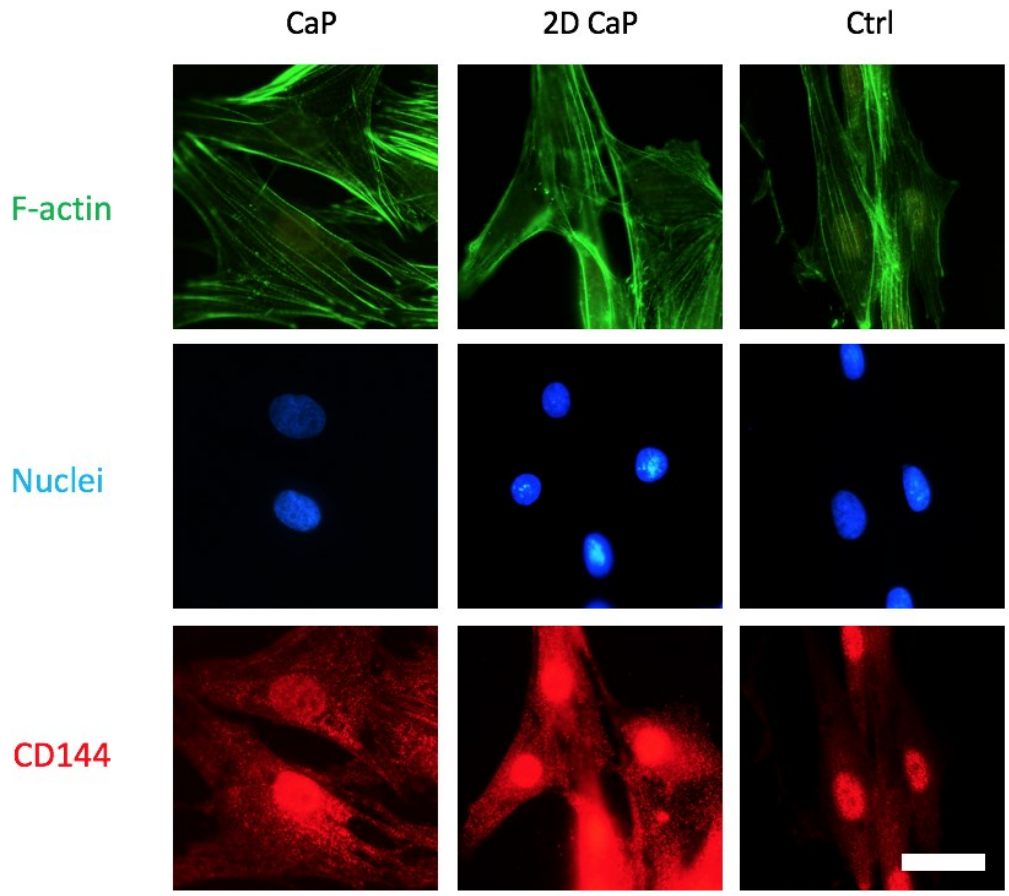

Figure S12 IF staining for the expression of polarization specific surface marker CD144 after the RAW 264.7 cells were incubated with indicated nanoparticles for 3 days. The proteins were stained with Cy3-labeled primary antibody against CD163 (red), nuclei were stained by DAPI (blue), and F-actin was stained with FITC labeled phalloidin (green). Scale bar = 50 μm.

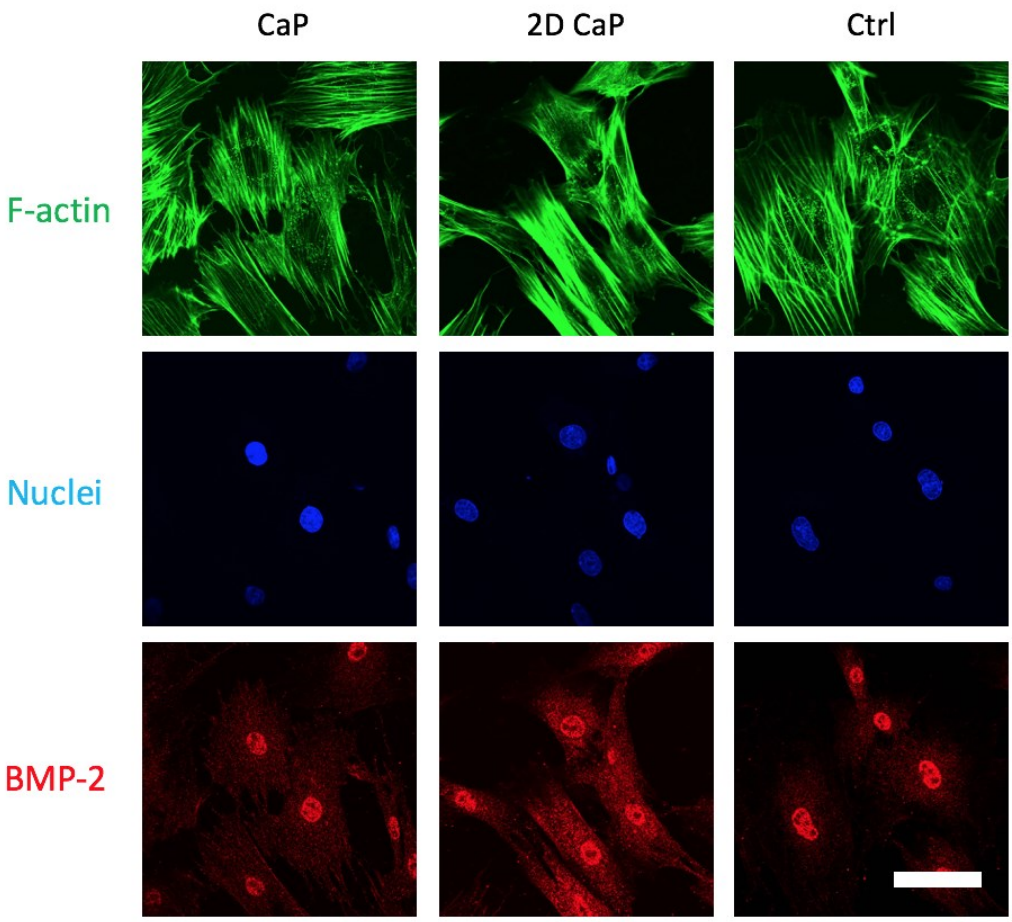

Figure S13 IF staining for the expression of polarization specific surface marker BMP-2 after the RAW 264.7 cells were incubated with indicated nanoparticles for 3 days. The proteins were stained with Cy3-labeled primary antibody against CD163 (red), nuclei were stained by DAPI (blue), and F-actin was stained with FITC labeled phalloidin (green). Scale bar = 50 μm.